Title
Role of Distortion Energy and Steric Effects on Cycloadditions in Bioorthogonal Chemistry

Author
Lopez, Steven Alexander

Publication Date
2012

Peer reviewed|Thesis/dissertation

UNIVERSITY OF CALIFORNIA

Los Angeles

Role of Distortion Energy and Steric Effects on Cycloadditions in Bioorthogonal Chemistry

A thesis submitted in partial satisfaction of the requirements for the degree of Master of Science in Chemistry

by

Steven Alexander Lopez

2013

ABSTRACT OF THE THESIS

Role of Distortion Energy and Steric Effects on Cycloadditions in Bioorthogonal Chemistry

by

Steven Alexander Lopez

Master of Science in Chemistry

University of California, Los Angeles, 2013

Professor Kendall N. Houk, Chair

The 1,3-dipolar cycloaddition and Diels-Alder reaction have been applied countless times in synthetic organic chemistry, materials chemistry, and now chemical biology. The stereoselectivity and rapid kinetics have been harnessed to develop the field of bioorthogonal chemistry. In this thesis, the origins of the rapid kinetics and exo-facial

selectivity of norbornene was explained and extended to a series of pyramidalized norbornenes and sesquinorbornenes. These were studied using DFT (Density Functional Theory) at the M06-2X/6-311G(d,p) level along with other computational models. The transition structures and activation barriers for these reactions were calculated. An analysis of the calculations revealed that distortion energy is greatly responsible for the observed stereoselectivity, and a simple relationship was derived between pyramidalization and activation barriers. We propose the term, distortion-accelerated, to describe why the reactions are fast, rather than strain-promoted, because the alkenes release most of their strain energy before the transition state.

In a second portion of the thesis I applied the concept of distortion-acceleration to a recently discovered mutually orthogonal 1,3-dipolar cycloaddition and an inverse-demand Diels-Alder reaction. Mutually orthogonal reactions were used in the literature to selectively label two different cancer cells simultaneously. We explained this selectivity difference using modern computational methodology. DFT was used for this computational investigation at the M06-2X/6-311+G(d,p) level and the Polarizable Continuum Model (PCM) was used to correct for solvation effects. It was found that distortion energy, LUMO energies, and steric effects are responsible for the observed selectivity. General rules were developed to easily predict new mutually orthogonal pairs once their bioorthogonality is known.

The thesis of Steven Alexander Lopez is approved.

Neil K. Garg

Miguel A. Garcia-Garibay

Kendall N. Houk, Committee Chair

ACKNOWLEDGEMENTS AND DEDICATION

I would like to thank Professor Houk for his commitment and support in my research. Also, I would like to thank Dr. Peng Liu for helping me through the first steps of computational chemistry and continued assistance throughout my time at UCLA. Dr. Yong Liang has provided invaluable discussions to decode bioorthogonal reactivity and selectivity.

To Manuel and Teresa Lopez

Table of Contents

Role of Distortion Energy and Steric Effects on Cycloadditions in Bioorthogonal Chemistry

LIST OF FIGURES

LIST OF SCHEMES

LIST OF TABLES

I. Introduction

1,3-dipolar cycloadditions are among the most useful reactions in synthetic organic chemistry; Huisgen described the concept and discovered many examples in the 1960s. One important type of 1,3-dipolar cycloaddition involves azides as 1,3-dipoles. Huisgen observed that norbornene reacts with phenyl azide 5–200x faster than strain energy release would predict.[1,2] The activation barrier was 1-3 kcal/mol lower than predicted by strain release, and referred to this mysterious factor responsible for lowering the activation barrier as factor "*x*". In addition, the reaction was stereoselective, as are many additions to norbornene greatly favoring the exo cycloadduct. In this century, the concept of "click chemistry" was proposed by Sharpless.[3] Click reactions are a category of reactions that proceed in high yield under mild conditions, producing "inoffensive" or no side products, and are done in "green" solvents. The 1,3-dipolar cycloaddition that Sharpless describes as a "click reaction" involved allylic azides and terminal alkynes; these reactions proceed at room temperature with a Cu(I) catalyst. Most recently, several groups have applied the 1,3-dipolar "click" reaction to biological systems. Bertozzi, the pioneer of this field, coined the term "bioorthogonal reaction" in 2003 to describe a

reaction that occurs in a biological setting without disrupting the normal functions of the system.[4] The azide-alkyne click reaction is ideally suited for this field, because alkynes and azides do not occur as functional groups in biological systems. Bertozzi first introduced the "Cu-free Click Reaction" which involved strained cyclooctynes and benzyl azide. The inherent strain energy of the cyclic alkyne raises the energy of the reactant and eliminates the need for the toxic Cu(I) catalyst. In early 2012 Hilderbrand et al. introduced the concept of mutually orthogonal bioorthogonal reactions.[5]

This thesis describes a computational exploration of the stereoselectivity of norbornene cycloadditions, defines and expands upon the concept of distortion-accelerated reactions and how they differ, at least conceptually, from 'strain-promoted' reactions. This introductory chapter contains a synopsis of the two publications that have resulted from this research. Part I involves the transition states of the (3 + 2) cycloadditions of phenyl azide with a series of very strained alkenes (Figure 2) calculated using DFT.

Part II introduces the concept of bioorthogonal and mutually orthogonal bioorthogonal reactions and the many applications of this relatively new technique to label biomolecules.

II. Background

The 1,3-Dipolar Cycloaddition

The 1,3-dipolar cycloaddition, described by Huisgen in the 1960s was studied extensively in his laboratory.[6] This reaction, is a pericyclic reaction and follows the symmetry rules developed by Woodward and Hoffmann.[7] The 1,3-dipolar cycloaddition, like the Diels-Alder reaction[8] is stereospecific due to the concerted mechanism. Cycloadditions have the nomenclature which is specified by the number of π electrons and follows the format [a + b], where a represents the larger number of π electrons. 1,3-dipolar cycloadditions and Diels-Alder reactions are both [4+2] cycloadditions. It is also correct to use parenthesis instead of brackets when citing the number of atoms taking part in the cycloaddition (a + b). Thus, the 1,3-dipolar cycloaddition is also described as (3+2) cycloaddition.

Norbornenes

Norbornene (bicyclo[2.2.1]heptene) is a strained bicyclic hydrocarbon, the IUPAC naming in brackets refers to the number of carbons bound to bridgehead carbons. The existence of the norbornyl non-classical cation was famously debated for many years by Winstein and Brown in the 1950s. Huisgen showed that norbornene reacted with phenyl azide much than expected with phenyl azide based on its intrinsic strain energy. It was also shown that the reaction was stereoselective; only an exo cycloadduct could be isolated upon heating in the presence of phenyl azide.[6] This *extra* reactivity was equal to a lowering of the activation barrier by 1-3 kcal/mol and was called factor "*x*". Early calculations by the Houk group determined that torsional steering was responsible for the enhanced reactivity and stereoselectivity observed by Huisgen twenty years prior.[9]

The sesquinorbornene is a molecule consisting of two fused norbornenes at the double bond. *Syn* and *anti*-sesquinorbornene are stereoisomers. In a mechanistic study by Bartlett et al., their reactivity towards phenyl azide and other reagents were explored. Structural data was extracted from X-ray crystallography, revealing a non-planar double bond in *syn*-sesquinorbornene and norbornene. *Anti*-sesquinorbornene was found to have a planar double bond. Rate constants were measured for the (3+2) cycloaddition of phenyl azide to the sesquinorbornenes and norbornene.[10]

2.2 Pyramidalization of Alkenes

Previous studies have shown that ring strain and ground state angle distortion contribute greatly to the extent of alkene pyramidalization.[11, 12, 13] Second-order Jahn-Teller distortion, leads to stabilization resulting from mixing of 2s orbitals of the alkene carbons with p orbitals which form the π bond.[14] Pyramidalization occurs in the endo direction for norbornene derivatives to minimize torsional strain.[20]

2.3 Bioorthogonal Chemistry

A bioorthogonal reaction is a reaction whose components nor the products interfere with cellular processes and viability. For the reaction to be 'bioorthogonal' the functional groups must have chemical complementarity and cannot have competing side reactions in biological systems. Functional groups such as phosphines, azides, and alkynes are typical functional groups used in bioorthogonal reactions. The earliest example of a bioorthogonal reaction was reported in 2000 by Bertozzi and co-workers;[15] it was based on the classic Staudinger reaction.[16] The generation of a water-unstable aza-ylide was problematic in biological systems, a methyl ester was incorporated to act as a nucleophile trap and the reaction proved to be bioorthogonal *in vitro*. (Figure 1)

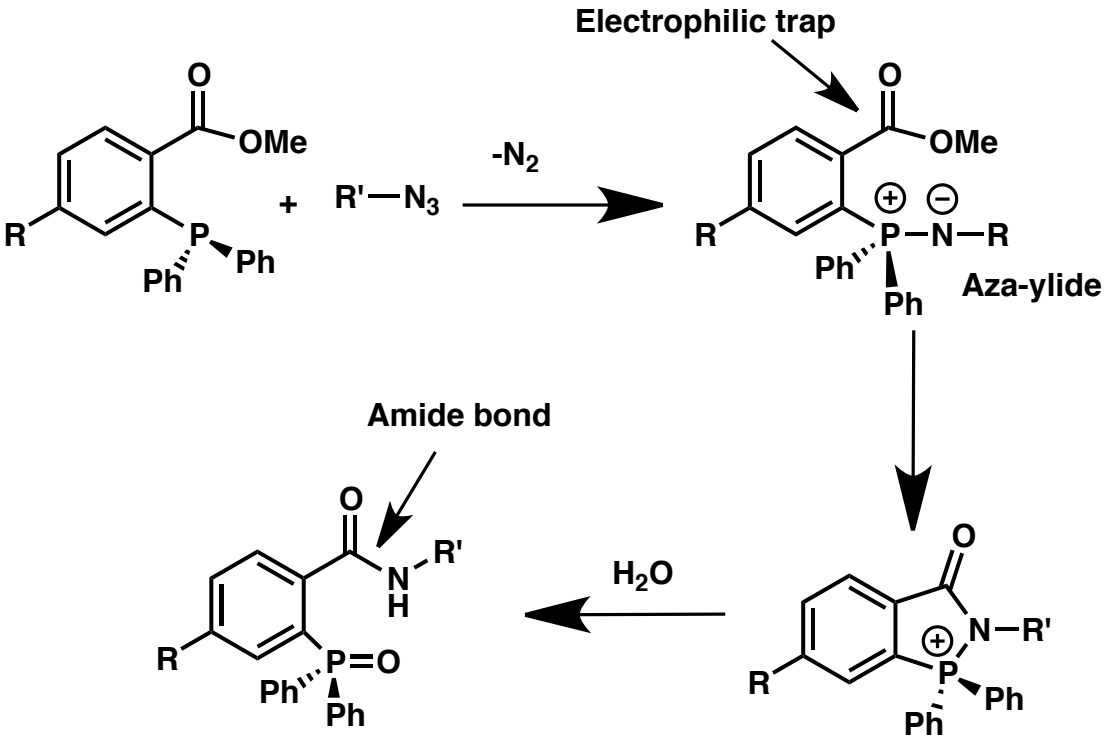

Figure 1. The first bioorthogonal reaction, the Staudinger Ligation as reported by Bertozzi group.

III. Computational Methods

All computations were carried out with the GAUSSIAN 09 series of programs.[17] Reactants, transition states, and products were optimized with the M06-2X[18] functional. Vibrational analysis confirmed all stationary points to be minima (no imaginary frequencies) or first order saddle points (one imaginary frequency). An ultrafine grid was used with the M06-2X/6-311+G(d,p) geometry optimization. Frequency calculations on these stationary points provided activation enthalpies and free energies. Additional electronic energies using SCS-MP2 [19] /6-311G+(d,p)//M06-2X/6-311G+(d,p). A Conductor-like Polarizable Continuum Model (CPCM) [20,21] for solvation by water single point calculation was used for the computations. A quasiharmonic correction was applied during the entropy calculations by setting all frequencies to 100 cm^{-1} when they are less than 100 cm^{-1}.[22,23]

3.1 Density Functional Theory

Density functional theory (DFT) is founded on the concept that the energy of a molecule is a function of its electronic density. This is in contrast to *ab initio*, semi-empirical, and wave function methods. A main advantage of DFT is its reduced cost to calculate electron correlation. DFT calculates the electron density function to then determine the energy of the ground state and other properties of an atom or molecule. DFT has proved to calculate geometries and energies relatively accurately.

3.2 Basis Sets

Quantum mechanics is built upon the concept that matter has both particle and wave characteristics. Matter and its vibrations are represented by wave functions, which can be solved using the Schrödinger equation. Atomic orbitals, volumes around atoms where electron density can be found, are derived from these wave functions. Linear combinations of these atomic orbitals result in molecular orbitals, orbitals that describe the electron density of the molecule. Quantum mechanical computations involve approximate solutions of the Schrodinger equation. The Gaussian-Type Orbital (GTO) is not an adequate approximation for wave functions on their own. However, a combination of multiple GTO functions result in a much better approximation of the wave function. A basis set is a set of these basis functions that approximates atomic orbitals of atoms in a molecule and the molecular orbitals after the linear combination of these orbitals.

3.2.1 *6-311+G(d,p)*

Valence orbitals in the 6-311+G(d,p) basis set are split into inner and outer shells. The "G" simply means that GTO functions are being used. The first number in this nomenclature, 6, is a function describing inner shell orbitals (e.g. 1s orbital is on C, N, O) of each core orbital with the number of primitive Gaussian functions. The next two numbers indicate that the valence orbitals are composed of two basis functions each. The second number, 3 is a linear combination of three primitive Gaussian functions describing inner shell orbitals. The next numbers, 1, describe the middle and outer

valence orbitals using one Gaussian function. Describing the middle and outer orbitals shells is considered a *split-valence triple-zeta* basis set. The "+" denotes a *diffuse function* that is also being calculated. Diffuse functions extend orbital sizes beyond their typical size to account for electron density found further from the nucleus than normal. This function was used due to the presence of lone pair electrons on the compounds undergoing bioorthogonal cycloaddition reactions. The first letter (d) in the parenthesis following the "G" describes d orbitals on "heavy" atoms with p orbitals in their valence shell such as C, N, O. The second letter (p) applies to atoms with only s orbitals in their valence shell ("light atoms"). By adding higher-level orbital functions, polarization of the orbital can occur in these computations.

3.3 Self-Consistent Reaction Field Methods for Solvation

Many of the calculations in this thesis are done in the gas phase, but the reactions we are modeling are performed in various solvents. Solvation calculations are used to compute approximate solvation energies. The Self-Consistent Reaction Field (SCRF) method known as the Polarized Continuum Model. An SCRF, such as PCM, is a uniform continuum of the dielectric constant (ε), of the solvent. The transition structure or reactant is positioned inside of a corresponding cavity in this uniform field. The PCM model treats the solute cavity as a fusion of overlapping atomic spheres within a numerically calculated polarized solvent field.

3.4 Intrinsic Reaction Coordinate

The *Intrinsic Reaction Coordinate* (IRC) is one path out of many that connect two minima on the potential energy surface. IRC calculations begin at the transition structure and systematically "steps" down each side of the reaction coordinate to either minimum. This technique is useful to prove a transition structure corresponds to the reactants and product in the reaction of interest.

IV. Synopsis of Publications

4.1 "Alkene Distortion Energies and Torsional Effects Control Reactivities and Stereoselectivities of Azide Cycloadditions to Norbornenes"
Lopez, Steven Alexander; Houk, K. N. *J. Org. Chem.* **2012**, 10.1021/jo301267b

This work is a computational investigation of the 1,3-dipolar cycloaddition between a series of norbornenes and phenyl azide. The work utilized modern computational methods employing density functional theory with Truhlar's hybrid functional, M06-2X with a triple zeta basis set. A benchmarking paper by our group shows that the M06-2X functional predicts cycloaddition activation barriers very close to experimental ones.[24] The distortion/interaction model, was used to explain the stereoselectivity and reactivity of the norbornenes. The focus of the paper was to explain the overwhelming exo facial stereoselectivity and to describe the origins of its reactivity towards 1,3-dipoles. In addition to norbornene we studied *syn*- and *anti*-sesquinorbornene and a series of norbornenes to understand what causes the stereoselectivity and accelerated reaction rates. Unstrained *cis*-alkenes **1** and **2** were used as standards to which the norbornenes could be compared.

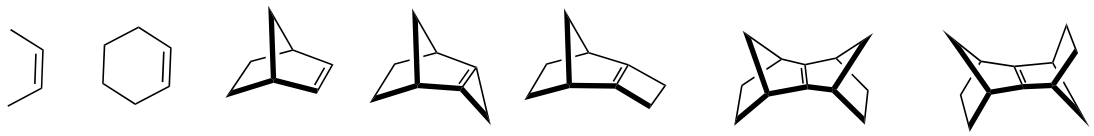

1 **2** **3** **4** **5** **6** **7**

We verified that the double bonds in alkenes **3** – **6** are pyramidalized in the endo direction. This has been published experimentally, and the alkenes optimized by M06-2X closely matched crystal structures of these alkenes. Pyramidalization proved to play a key role in the stereoselectivity of these reactions. Thus, the reactants are *pre-distorted* to resemble the exo transition structures. Less distortion energy is required to reach the transition state geometries. The endo transition states require much higher distortion energy is required to reach the transition state geometries. The interaction energy is identical for the exo and endo transition structures. The preferred exo attack has staggering about the forming bonds, while endo attack is eclipsed and higher in energy.

We do not find any correlation between activation enthalpy and reaction enthalpy for the reactions in this study. The distortion-accelerated reactions release strain primarily from the reactants to the transition state, which correlates with faster rates. We have discovered a linear relationship between the activation enthalpy and the extent of pyramidalization of the alkene.

4.2 Origins of Bioorthogonal and Orthogonal Cycloadditions: Distortion, LUMO Energies, and Steric Effects

Yong Liang, Joel Mackey, Steven Alexander Lopez, Acia Liu, K. N. Houk*
J. Am. Chem. Soc. **2012**, *134*, 17904.

This work was a collaborative project with a subgroup in the Houk group, and my contribution is described below. The focus of this paper was to explain the selectivity of mutually orthogonal bioorthogonal cycloaddition reactions. Green Fluorescent Protein (GFP) is widely used to tag proteins to study expression and localization in cells because it is relatively easy to genetically encode. However, its relatively large size often cases structural perturbations to the protein being studied and limits the target biomolecule to proteins since it must be genetically encoded. Bioorthogonal reactions allow specific and rapid reactions to take place to tag biomolecules such as cell-surface glycans, lipids, and nucleic acids. In a publication by Hilderbrand this year, two different cancer cells were concurrently labeled using a pair of mutually orthogonal bioorthogonal reactions.[5]

We used the Truhlar M06-2X hybrid functional to investigate the selectivity shown by Hilderbrand. We employ the distortion/interaction model to dissect the activation barriers into the distortion and interaction terms, which helped to provide a set of general rules to predict new bioorthogonal reactions. My contribution to this work was to calculate the activation barriers for the (3+2) cycloaddition of *trans*-cyclooctene and

methyl azide. The inverse-electron demand Diels-Alder reaction is experimentally shown to proceed 33,000 times faster than the azide cycloaddition. The highly strained *trans*-cyclooctene was used because the reaction with the tetrazine or azide is distortion-accelerated. However, this alone cannot explain the extremely fast reaction of *trans*-cyclooctene with tetrazine. Interaction energy was shown to account for the difference in reactivity. The frontier molecular orbitals were computed for methyl azide, dimethyl tetrazine, and *trans*-cyclooctene to compare their energies. The smallest HOMO-LUMO gap occurs when comparing the energies of the alkene HOMO and the dipole and diene LUMO. The tetrazine is considerably more electrophilic than methyl azide, which lowers the LUMO energy and reduces the HOMO-LUMO gap.

Hilderbrand reports that dibenzocyclooctyne (DIBO) reacts quickly with azides, but not at all with tetrazines. In light of the tetrazine results with *trans*-cyclooctene, we sought to explain this selectivity. Consistent with the *trans*-cyclooctene results, larger interaction energy resulted from cycloaddition with tetrazine over methyl azide. However, the distortion energy was significantly higher to reach this transition state geometry. A significant steric clash of the methyl and benzylic hydrogens occurs in the transition state. The relatively large size of tetrazine prohibits tetrazine from approaching with its LUMO aligned with the reacting alkyne π bond. Tetrazine approaches the alkyne at an angle in the transition state, which directly reduces orbital overlap.

Understanding cycloaddition reactivity allows chemical biologists to predict new reaction pairs and to fine-tune the reactivity based on the simple rules we have provided.

Electronic effects resulting from a low-lying LUMO on the 4π compound can greatly accelerate reactions when there are no competing steric effects. Steric clashes can override electronic effects for reactions with sterically hindered 2π compounds.

V. Results and Discussion: Alkene Pyramidalization Publication

The following section has been published, Lopez, Steven Alexander; Houk, K. N. *J. Org. Chem.* **2012**, DOI: 10.1021/jo301267b.)

We report computed transition structures and activation barriers for cycloadditions to a number of norbornenes and to the simple alkenes, *cis*-2-butene (**1**) and cyclohexene (**2**). In addition to norbornene, tricyclic hydrocarbons with norbornene fused to cyclopropene or cyclobutene, (**4** and **5**) *syn*-sesquinorbornene (**6**), and *anti*-sesquinorbornene (**7**) were studied. These compounds are shown in Figure 2. The unstrained planar alkenes (**1**, **2**) are used as a standard to which the reactivity of pyramidalized alkenes (**3**-**6**) can be compared. The results of this study inspired further study where the origins of reactivity and selectivity of bioorthogonal reactions was explored using distortion/interaction model. The details of this work are explained in Part II of the thesis.

1 **2** **3** **4** **5** **6** **7**

Figure 2. Series of dipolarophiles studied

The optimized structures of alkenes **3**-**6** are shown in Figure 3. The ideal bond angle for sp^2 hybridized carbons is 120º, while sp^3 carbons have an ideal bond angle of 109.5º; consequently, the smaller C-C=C angles in strained alkenes reduce the force constants for out-of-plane bending. We use d_{ish} to quantify the degree of pyramidalization in these alkenes. The torsional angle, θ, designated by the green atoms of **3** in Figure 3 is subtracted from 180º to obtain the out-of-plane bending angle, θ_{dih}. θ_{dih} = 0º when θ = 180º. This value is identical to the 'butterfly angle' (ψ), as described by Williams.[25] θ_{dih} is 60º for a perfectly sp^3 pyramidalized alkene. Our high-level DFT calculations compare well with previous results by Vazquez,[26] Williams,[20] and our group.[9] We report θ_{dih} of 8°, 45°, 21°, 16°, and 0° for alkenes 3, 4, 5, 6, and 7, they report 7°, 44°, 18°, 16°, and 0° for the same alkenes.

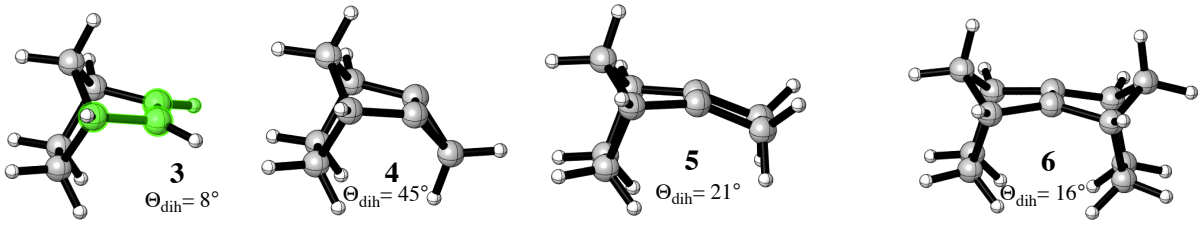

Figure 3. Optimized minima of **3**, **4**, **5**, and **6** as calculated by M06-2X/6-311G(d,p). The green atoms in 3 define θ_{dih}.

5. 1 Distortion/Interaction Model

The distortion/interaction model was developed by our group[27] and is similar to the activation strain model proposed by Bickelhaupt[28]. The distortion/interaction model is shown in Scheme 1 and is used to further understand the reactivity of bimolecular reactions by dissecting the activation barrier ($\Delta E^{\ddagger}$) into two components: distortion and interaction energies. Distortion energy ($\Delta E_d^{\ddagger}$) is sum of energy required to distort each of the fragments from their equilibrium geometries to their respective transition structure geometries at an infinite distance from each other. Interaction energy ($\Delta E_i^{\ddagger}$) is a generally stabilizing energy that results from favorable orbital interactions and electrostatics. Distortion energy is calculated by isolating each of the fragments and performing a single-point calculation on each fragment. Interaction energy is a generally stabilizing interaction that results from the overlap of orbitals in the transition state.

Scheme 1. The distortion/interaction model.

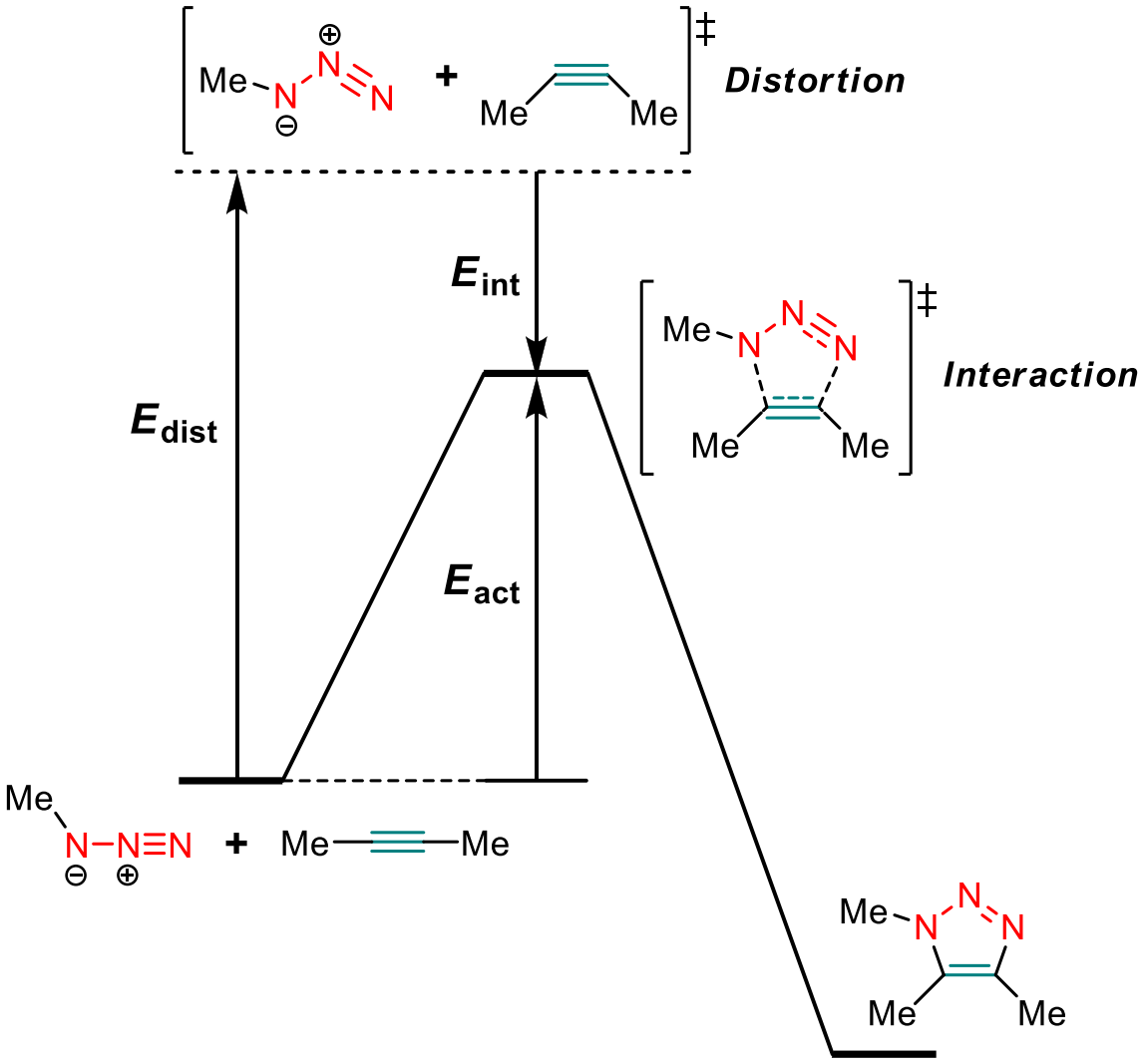

The optimized transition structures of the 1,3-dipolar cycloaddition of phenyl azide to dipolarophiles **1** – **7** are in Figure 4. The reactions are concerted, but the transition structures show that bond formation is slightly asynchronous. The dipolarophiles in the transition states all have nearly identical alkene bond lengths (1.35 Å - 1.39 Å). However, the ∠NNN and forming bond distances between the dipole and dipolarophile vary significantly through the series, 136 - 153º and 2.08 – 2.49 Å, respectively. The partial bond to the more electrophilic (unsubstituted) terminus of phenyl azide is somewhat shorter than the partial bond to the more nucleophilic terminus.

The transition structures for the planar alkenes, cis-2-butene (**1**) and cyclohexene (**2**) are very similar, with ∠NNN of 137º and 136º, respectively. Both have average forming C-N bond lengths of 2.14 Å. Anti-sesquinorbornene is planar and has an earlier transition state, the result of increased steric clashes in the transition structure between the ethylene bridges of syn-sesquinorbornene. The exo transition structures for the norbornenes (**3-6)** have NNN angles that increase with increasing θ_{dih} in the reactants; this correlates with the lower activation barriers and earlier transition states as θ_{dih} increases. The exo transition structures for the reactions of **3**, **5**, and **4** with phenyl azide have ∠NNN = 139º, 144º, and 150º, respectively, and correspond to increasingly early transition states.

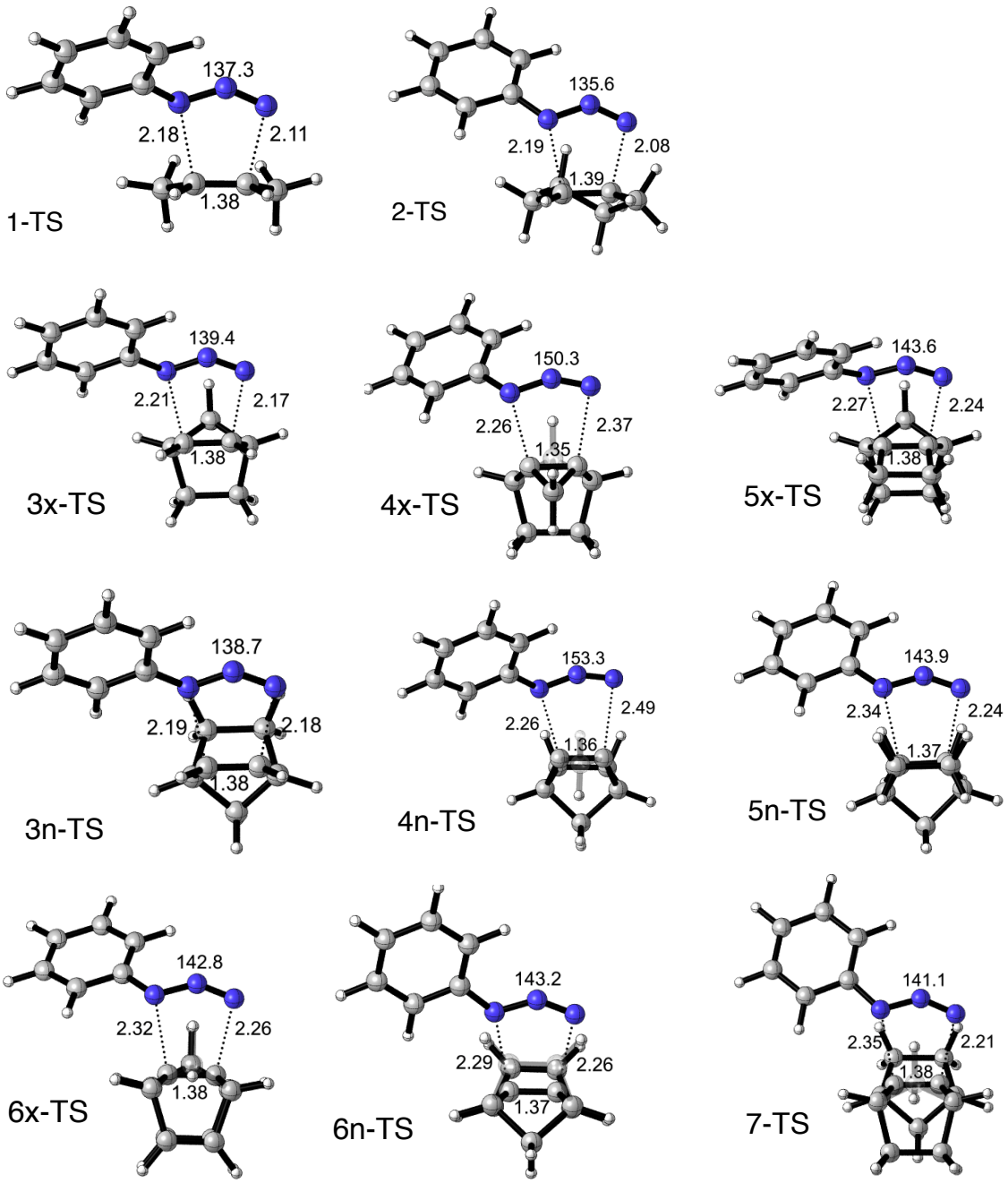

Figure 4. Optimized transition structures of the 1,3-dipolar cycloaddition of phenyl azide to alkenes **1**-**7** as calculated by M06-2X/6-311G(d,p). Bond lengths are reported in Å

5.2 Stereoselectivities

The exo stereoselectivity seen in these reactions results from different torsional effects in exo and endo transition states. Figure 5 shows Newman projections along the 1,2 and 3,4 bonds in the 1,3-dipolar cycloaddition transition states of norbornene and phenyl azide. These torsional effects are representative of all of the pyramidalized alkenes discussed here. A nearly perfect staggered conformation about the C-1, C-2 bond can be seen for the exo transition structure (**3X-TS)** on both termini of phenyl azide. The Newman projections for the endo cycloaddition of phenyl azide to norbornene show that the partially formed C-N bonds and the vicinal HCCH bonds suffer some eclipsing, while the $HCC_{bridged}H$ eclipsing is severe, a factor noted originally by Schleyer for norbornyl solvolysis.[29]

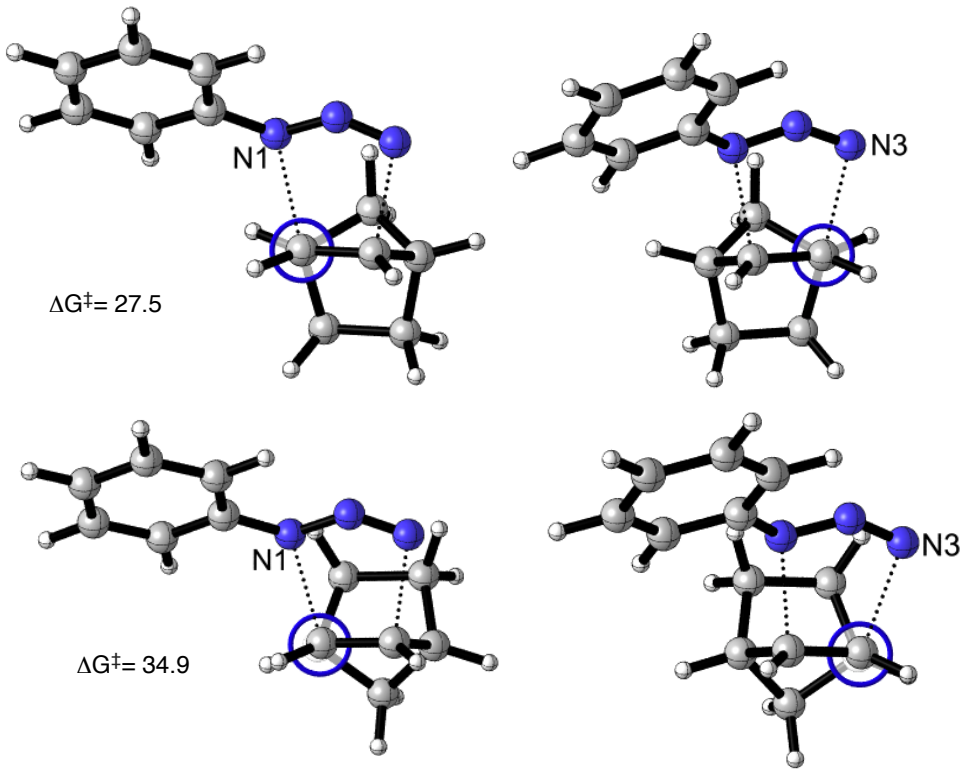

Figure 5. Newman projections for the cycloadditions of phenyl azide to the **3X-TS** (top row) and **3N-TS** (bottom row) faces of norbornene. $\Delta G^{\ddagger}$ values (kcal/mol) are shown below the Newman projections.

We first established that computed activation free energies correspond reasonably well to experiment values, when available. Table 1 shows a comparison of the experimental activation barriers to the computed barriers using M06-2X/6-311G(d,p) and SCS-MP2/6-311G(d,p)//M06-2X/6-311G(d,p). Both predict higher activation barriers than $\Delta G^{\ddagger}_{expt}$. Both give the correct order of reactants, but M06-2X gives an experimentally good correlation.

Table 1. $\Delta G^{\ddagger}_{expt}$ [a] , values derived from experimental rate constants. $\Delta G^{\ddagger}_{comp.}$ energies include solvation by CPCM (CCl_4 or Et_2O). The reactions of phenyl azide with dipolarophiles **2, 3,** and **7** as calculated by M06-2X/6-311G(d,p), and [SCS-MP2/6-311G(d,p)//M06-2X/6-311G(d,p)]. Linear regressions are shown below the table.[c]

alkene	Solvent	T (°C)	$10^7 k_2$ ($M^{-1}s^{-1}$)	$\Delta G^{\ddagger}_{expt}$ [a,b] (kcal/mol)	$\Delta G^{\ddagger}_{M06\text{-}2X}$ (kcal/mol)	$\Delta G^{\ddagger}_{SCS\text{-}MP2}$ (kcal/mol)
Cyclohexene[30]	CCl_4	25°	0.03	29.0	33.1	32.1
Norbornene[35]	CCl_4	25°	188	23.9	28.2	29.0
Anti-sesquinorbornene[31]	Et_2O	30°	270	23.6	27.4	25.3

[a] Calculated from $k = 6 \times 10^{12} e^{(-\Delta G^{\ddagger}/RT)}$, derived in SI.
[b] Computed free energies in solution are for the standard state of 1M.[1,1]
[c] Linear Regression between $\Delta G^{\ddagger}_{calc}$ and $\Delta G^{\ddagger}_{expt.}$ for M06-2X and SCS-MP2 methods. M06-2X/6-311G(d, p) $\Delta G^{\ddagger}_{calc} = 1.01 \Delta G^{\ddagger}_{expt} + 3.72$; $R^2 = 0.99$ and SCS-MP2/6-311G(d,p)//M06-2X/6-311G(d,p) $\Delta G^{\ddagger}_{calc} = 0.97 \Delta G^{\ddagger}_{expt} + 4.05$; $R^2 = 0.75$.

Table 2 gives the computed activation barriers, ($\Delta G^{\ddagger}$, $\Delta H^{\ddagger}$, $\Delta E^{\ddagger}$) distortion and interaction energies, and the NNN angle in each transition structure studied here. There is a large range of activation energies, $\Delta E^{\ddagger}$ (3-27 kcal/mol) and a similarly large range of distortion energies, $\Delta E_d^{\ddagger}$ (12-38 kcal/mol), but a relatively small range of interaction energies, $\Delta E_i^{\ddagger}$ (8-14 kcal/mol). The distortion energies of the alkenes control barrier heights (Table 1), while the interaction energies are nearly constant. The range of alkene distortion energies (2-23 kcal/mol) is notably larger than the range of distortion energies of phenyl azide (15-25 kcal/mol), although the latter are generally larger than the former

Table 2. M06-2X/6-311G(d,p) activation free energies and enthalpies of activation, electronic energies of activation, distortion energies, and interaction energies for the reactions of phenyl azide and dipolarophiles **1-7**. (X=exo, N=endo) ∠NNN is the azide bond angle in each respective transition structure is represented by.

Alkene	$\Delta G^{\ddagger}$	$\Delta H^{\ddagger}$	$\Delta E^{\ddagger}$	ΔH_{rxn}	$\Delta E_d^{\ddagger}$ Alkene	$\Delta E_d^{\ddagger}$ PhN_3	$\Delta E_d^{\ddagger}$ Total	$\Delta E_i^{\ddagger}$	∠NNN (°)
1	32.8	19.6	19.1	-29.2	7.6	23.4	31.1	12.0	137.3
2	32.2	19.6	19.2	-26.8	8.2	25.1	33.3	14.1	135.6
3X	27.5	14.7	14.4	-38.1	4.6	20.5	25.0	10.7	139.4
3N	34.9	21.7	21.1	-36.5	10.8	21.1	31.9	10.8	138.7
4X	16.0	3.3	3.1	-68.6	0.9	10.6	11.5	8.4	150.3
4N	21.6	9.3	9.0	-71.9	9.0	8.2	17.2	8.2	153.3
5X	22.1	8.7	8.3	-51.0	2.5	16.4	18.9	10.6	143.6
5N	30.8	17.6	17.2	-53.7	12.6	15.1	27.7	10.5	143.9
6X	26.2	12.1	11.7	-33.4	3.9	21.2	25.1	13.4	138.8
6N	40.3	27.1	27.2	-41.3	22.6	15.7	38.3	11.1	143.0
7	26.4	13.8	17.6	-46.5	6.7	17.7	29.0	11.4	141.1

Figure 6 shows a plot of $\Delta E^{\ddagger}$ vs. $\Delta E_d^{\ddagger}$ for the seven reactions studied. There is an excellent linear correlation between distortion energy and activation energy ($r^2 = 0.96$). Similar relationships have been observed for the cycloadditions of many dipoles and dienes with simple alkenes.[32,33,34] and for related reactions by Bickelhaupt and coworkers.[35,36,] It was previously shown with 1,3-dipolar cycloadditions of acetylene and ethylene with many dipoles the distortion of the 1,3-dipole comprises ~80% of the distortion energy.[30] This portion of the total distortion energy is referred to as dipole distortion energy in this work and is defined as the energy required to bend the dipole into its transition structure geometry from its equilibrium geometry. In the azide cycloaddition studied here with unstrained **1** and **2**, dipole distortion energies, which comprise 75% of the total distortion energy. In the series of strained alkenes studied here, dipole distortion energy makes up 40-90% of the total distortion energy.

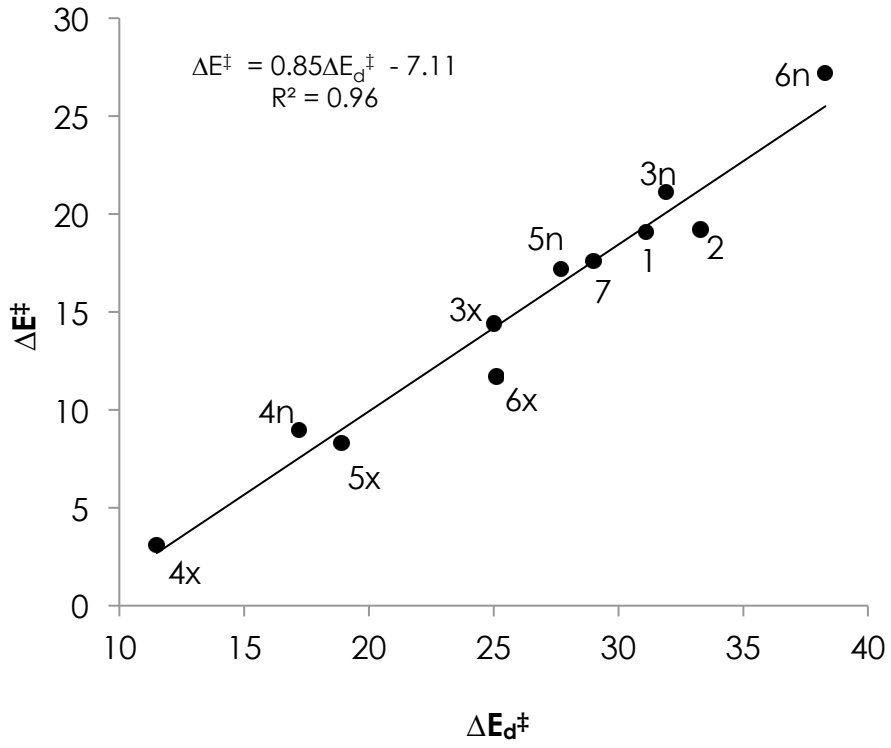

Figure 6. Plot of activation energies and distortion energies of the reactions of phenyl azide and dipolarophiles **1**-**7**, calculated by M06-2X/6-311G(d,p). Values in kcal/mol.

Despite the rather remarkable fit in Figure 6, two outliers, 6X and 6N are apparent. The activation barriers for the 1,3-dipolar cycloaddition of syn-sesquinorbornene deviate due to severe steric clashes in the endo transition structures. (Figure 4) This effect appears in the distortion energy as well. Pyramidalization plays a key role in the reactivity and stereoselectivity of these strained cycloalkenes undergoing 1,3-dipolar cycloadditions. The extent of pyramidalization (θ_{dih}) of the disubstituted alkenes (**1**-**5**) are first described, followed by the tetrasubstituted alkenes. (**6**-**7)** Norbornene (**3**) is the least pyramidalized alkene (θ_{dih} = 8º) and the $\Delta E^{\ddagger}$ of **3X-TS** is 14 kcal/mol, the highest among pyramidalized alkenes. The distortion energy of phenyl azide is similar for both transition states, but the large difference between alkene distortion energies favors the exo transition state (4.6 vs. 10.8 kcal/mol). The θ_{dih} of **5** is 21º and the $\Delta E^{\ddagger}$ drops to 8.3 kcal/mol. The lowered activation barrier is due to reduced distortion energy of the alkene and phenyl azide. The reduced distortion energy of phenyl azide is smaller and results from the earlier transition state involving the distorted alkene. The largest θ_{dih} is seen in the optimized structure of **4**, and the smallest $\Delta E_d^{\ddagger}$ and $\Delta E^{\ddagger}$ occur with **4X-TS** (11.5 and 3.1 kcal/mol, respectively). A remarkably small 0.9 kcal/mol is required to distort **4** into the exo transition state geometry, and 10.6 kcal/mol is required to distort phenyl azide into the NNN of 150º in the transition structure.

Syn-sesquinorbornene (**6**) has θ_{dih} = 16.8º; the distortion energies for **6X-TS** is 3.9 kcal/mol, and for **6N-TS** is 22.6 kcal/mol. The steric clashes of the hydrogens at carbons 3, 4, 8, and 9 with the azide contribute to the large difference in distortion energy, $\Delta\Delta E_d^{\ddagger}$

(13.2 kcal/mol) Anti-sesquinorbornene is planar like *cis*-2-butene and cyclohexene, but the transition state shows a greater ∠NNN than that of **1-TS** and **2-TS**. As a result, the dipole distortion energy is 6 kcal/mol lower than that of **1-TS**. The relatively early transition state requires less bending of phenyl azide, which results in a lower activation barrier. The $\Delta E^{\ddagger}$ for the reaction of tetramethylethylene with phenyl azide is 5.3 kcal/mol higher than for the reaction of anti-sesquinorbornene with phenyl azide. (Data in SI) The strained nature of the anti-sesquinorbornene compared to tetramethylethylene results in the lower distortion energy.

Figure 7 correlates pyramidalization (θ_{dih}) to reactivity ($\Delta H^{\ddagger}$) for the stereochemically-preferred reactions of **1**-**6** with phenyl azide. The planar alkenes, **1** and **2**, have nearly identical activation enthalpies. It is apparent that even slight pyramidalization of alkenes can greatly accelerate 1,3-dipolar cycloadditions. When $\theta_{dih} = 4°$, $\Delta H^{\ddagger}$ is lowered by 1.4 kcal/mol, which corresponds to an order of magnitude acceleration at 25 ºC. $\Delta H^{\ddagger}$ is 0 kcal/mol when the $\theta_{dih} = 51°$. For comparison, perfectly pyramidal sp^3 carbon has a corresponding θ_{dih} of 60°. It is notable that endo attack is also accelerated in the cases of high pyramidalization, compared to the unstrained alkenes. The degree of bending is an indication of the ease of out-of-plane bending and the magnitude of distortion energies. The role of strain release in controlling reactivity was investigated by comparing $\Delta H^{\ddagger}$ vs. ΔH_{rxn} in Figure 8. The energies of reaction used in this plot are shown in Table 1.

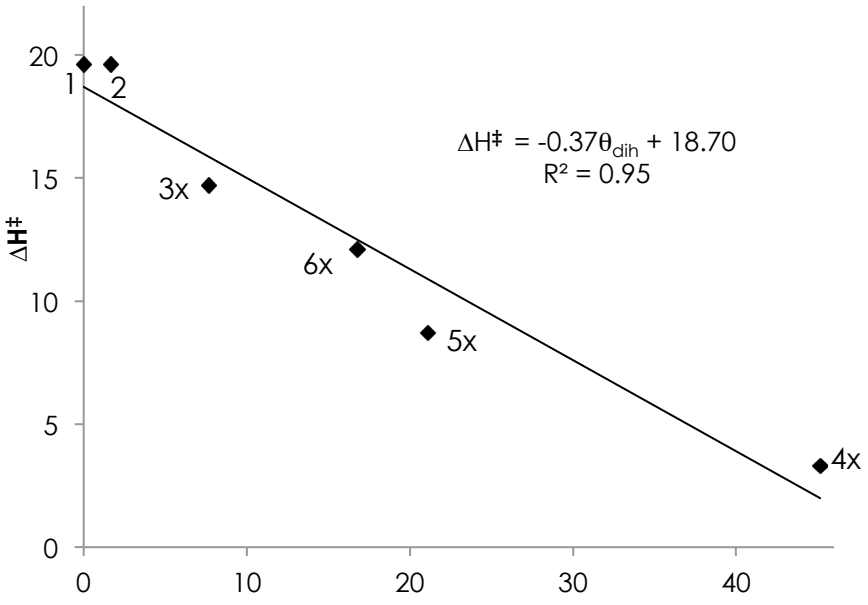

Figure 7. Plot of activation enthalpy (kcal/mol) vs. θ_{dih} (°), calculated with M06-2X/6-311G(d,p)

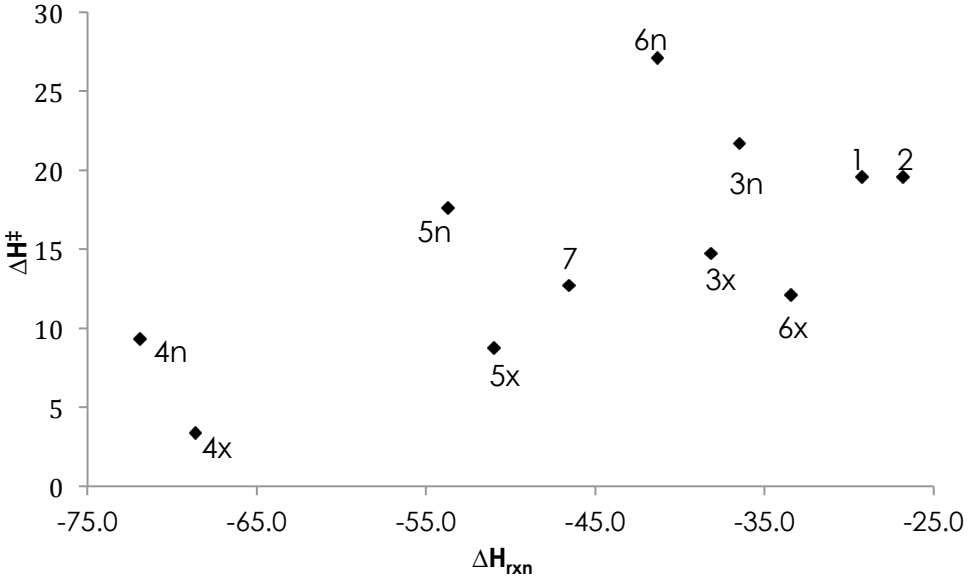

Figure 8. Plot of $\Delta H^{\ddagger}$ vs. ΔH_{rxn}, calculated by M06-2X/6-311G(d,p). $\Delta H^{\ddagger} = 0.30\,\Delta H_{rxn} + 28.61$; R^2=0.43.

There is no significant correlation of these quantities, and $R^2 = 0.43$. Consequently, there is no clear Dimroth, Brønsted, Evans-Polanyi, or Marcus relationship,[37,38,39] where the differences between activation barriers are about one-half of the differences in energies of reaction. Strain release, as measured by the change of energy upon reaction, shows only a qualitative relationship to reaction rates. In Figure 8, the most strain is released with the substrates on the left side of the graph, but only 4X shows unusually high reactivity. The lack of relationship between activation barrier and strain release indicates that the enhanced reactivities of these strained alkenes are not "strain-promoted". We have shown instead that they are distortion-accelerated when the ease of distortion to the transition state geometry is lowered.

VI. Part II: Origins of Selectivity in Bioorthogonal and Orthogonal Cycloadditions

I contributed significantly to the publication of this section, which was published. (Yong Liang, Y.; Mackey, J.; Lopez, Steven Alexander; Liu, A.; Houk, K. N. *J. Am. Chem. Soc.* **2012**, *134*, 17904.)

In 2004, the functional groups of azide and alkyne were brought together via a "strain-promoted click reaction" by Bertozzi using the strained eight membered ring, cyclooctyne.[40] The click reaction, as developed by Sharpless[41], had minor utility in living systems due to the toxic Cu(I) catalyst as required. Bertozzi and co-workers have developed strain-promoted (3+2) cycloaddition reactions between azides and cyclooctynes (Scheme 2a).[42]

Scheme 2. a) Azide-cyclooctyne (3+2) cycloaddition. b) *trans*-Cyclooctene-tetrazine (4+2) cycloaddition.

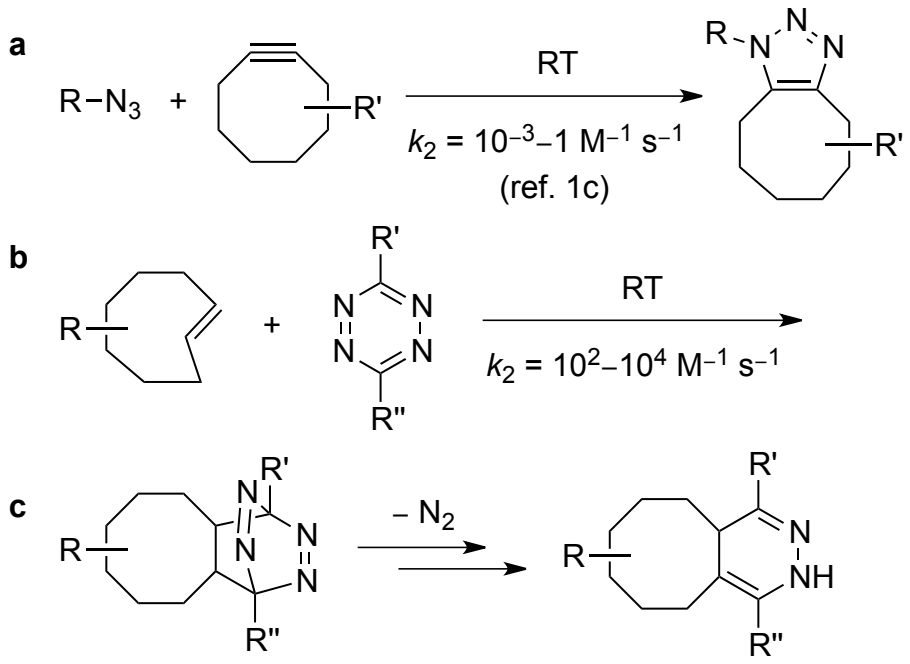

This "strain-promoted click reaction" proceeds at a rate that is sufficient for *in vivo* labeling without the toxic copper(I) catalysts traditionally employed in "click chemistry" involving azide cycloadditions. Several groups have developed a series of structurally varied cyclooctyne derivatives with different chemical reactivities and physical properties.[43] This strategy circumvented the copper toxicity problem. The strained cyclooctyne increases the energy of the dipolarophile relative to an unstrained dipolarophile, thus decreasing the amount of energy required to achieve the transition state geometry. The use of strain to raise the energy of the reactants and accelerate these cycloadditions has appeared in the literature many times in the last ten years. The first part of this thesis has utilized density functional theory (DFT) through modern computational methods to show that in fact these reactions are not "strain-promoted", but distortion-accelerated. These reactions are accelerated because the majority of the strain is released approaching the transition state, instead of to the products as is commonly described.

Another breakthrough in this area came in 2008 with applications of the inverse electron-demand Diels-Alder reactions of 1,2,4,5-tetrazines and strained alkenes (Scheme 1b).[44] In particular, the *trans*-cyclooctene-tetrazine (4+2) cycloaddition occurs with an extremely high bimolecular rate constant (k_2 = 10^2-10^4 M^{-1} s^{-1}),[45] much faster than the azide-cyclooctyne (3+2) cycloaddition (k_2 = 10^{-3}-1 M^{-1} s^{-1}).[1c] Hilderbrand and co-workers recently demonstrated that two bioorthogonal cycloaddition pairs can be mutually orthogonal.[8] As shown in Scheme 3a, *trans*-cyclooctene derivatives greatly prefer to

react with tetrazines rather than azides. On the contrary, dibenzocyclooctyne derivatives react with azides, but not with tetrazines under physiological conditions (Scheme 3b).

The mutually orthogonal bioorthogonal reactions allowed the researchers to concurrently distinguish two different cancer cells using this new technology. In this portion of the thesis, conclusive reasoning for the reactivity and selectivity of these reactions is presented. We have identified the origins of this extraordinary selectivity and have found why reactivity patterns of azides and tetrazines can be completely reversed by the appropriate choice of the 4π-ophile. At almost the same time, Schultz, Lemke, and co-workers found that *trans*-cyclooctenes show extremely high selectivity toward tetrazines rather than azides in protein labeling experiments.[46] However, the cyclooctyne-modified proteins couple with both tetrazine-functionalized and azide-functionalized dyes.[47] The similar reactivity of cyclooctynes with azides and tetrazines is also demonstrated by separate kinetic studies of the Bertozzi and Wang groups: tetrazines react with cyclooctynes only 1 to 2 orders of magnitude faster than azides do (Scheme 3c).[48] *Trans*-cyclooctene, cyclooctyne, and dibenzocyclooctyne are all highly strained molecules, but why do their selectivities toward azides and tetrazines in bioorthogonal cycloadditions differ dramatically? The answer to this question described here, provides a path to the future rational design of new bioorthogonal reactions. The close agreement between our predicted rates and the observed rates shows that computational methods are capable of reliable design predictions for development of additional usefully orthogonal cycloadditions based upon tuning of distortion, LUMO energies, and steric effects.

Scheme 3. Selectivity of bioorthogonal cycloaddition reactions. R-N_3 = AF647-azide, R^1 = Me, R^2 = $(CH_2)_5NH_2$, R^3 = PEG_4CO_2H, R^4 = CH_2Ph-(*p*-CO_2H) (for azide-cycloaddition) or H (for tetrazine-cycloaddition), R^5 = Bn, and R^6 = Ph.

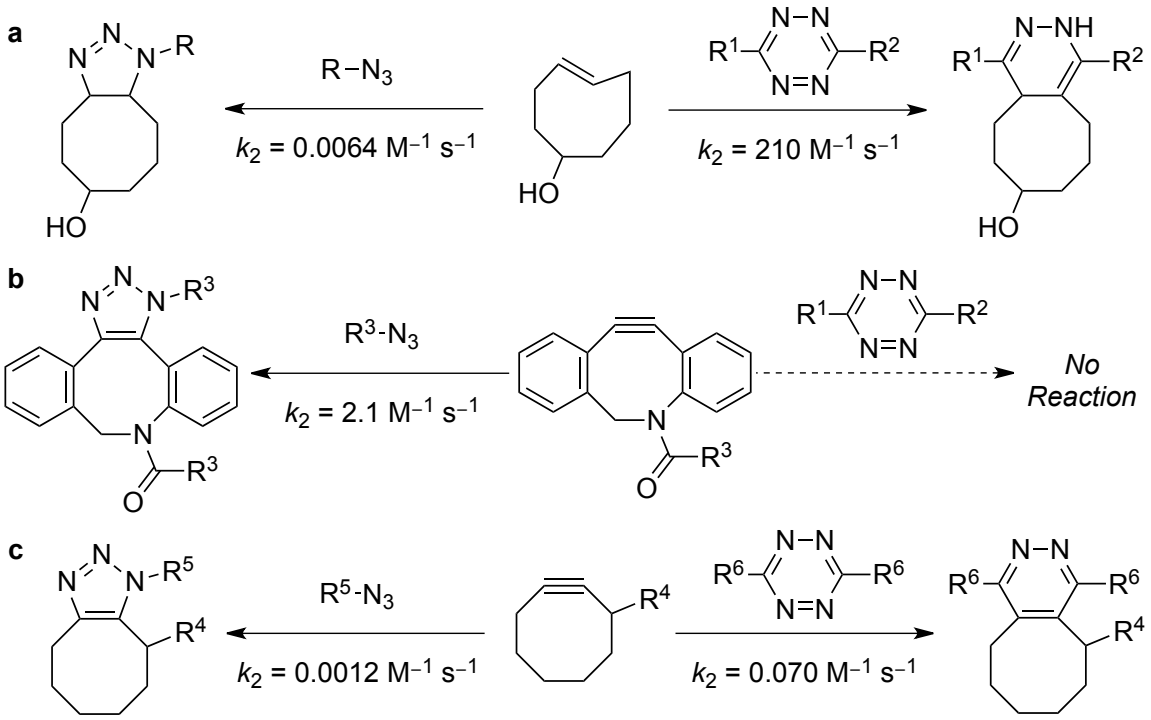

Table 3. M06-2X/6-311+G(d,p) computed activation free energies in the gas phase and in water (G_{gas} and G_{water}, in kcal mol^{-1}), relative rate constants (k_{rel}, based on G_{water} at 298 K), and activation, distortion, and interaction energies (E_{act}, E_{dist}, and E_{int}, in kcal mol^{-1}).

	G_{gas}	G_{water}	k_{rel}	E_{act}	E_{dist}	E_{int}
TS1	25.0	26.4	2.0	12.3	20.5 (17.8)[a]	-8.2
TS2	18.6	17.9	3.4×10^{6}	2.1	19.9 (16.4)[b]	-17.8
TS3	25.0	26.8	1.0	11.7	20.6 (17.9)[a]	-8.9
TS4	24.5	24.2	81	8.0	26.0 (20.3)[b]	-18.0
TS5	21.9	23.9	1.3×10^{2}	7.7	20.4 (17.1)[a]	-12.7
TS6	31.4	33.4	1.4×10^{-5}	13.7	36.7 (27.8)[b]	-23.0

[a] The data in parentheses are the distortion energies of methyl azide. [b] The data in parentheses are the distortion energies of dimethyltetrazine.

Computational Methodology

We have explored the cycloaddition reactions of *trans*-cyclooctene, cyclooctyne, and dibenzocyclooctyne with both methyl azide and dimethyltetrazine using quantum mechanical calculations.[49] M06-2X,[50] a density functional that we have shown to give relatively accurate energies for cycloadditions,[51] is used in this computational study. We also analyze the activation barriers of these reactions by using the distortion/interaction model.[52] In this model, the activation energy (E_{act}) of a reaction is analyzed in terms of the distortion energy (E_{dist}), the energy required for the geometrical deformation of reactants to achieve their transition state conformations, and the interaction energy (E_{int}), arising from the interactions between two distorted reactants in the transition state.

Results

Figure 9 shows the transition structures (**TS1-6**) for six investigated cycloaddition reactions. The computed activation free energies, relative rate constants, and the distortion/interaction energies are summarized in Table 3.

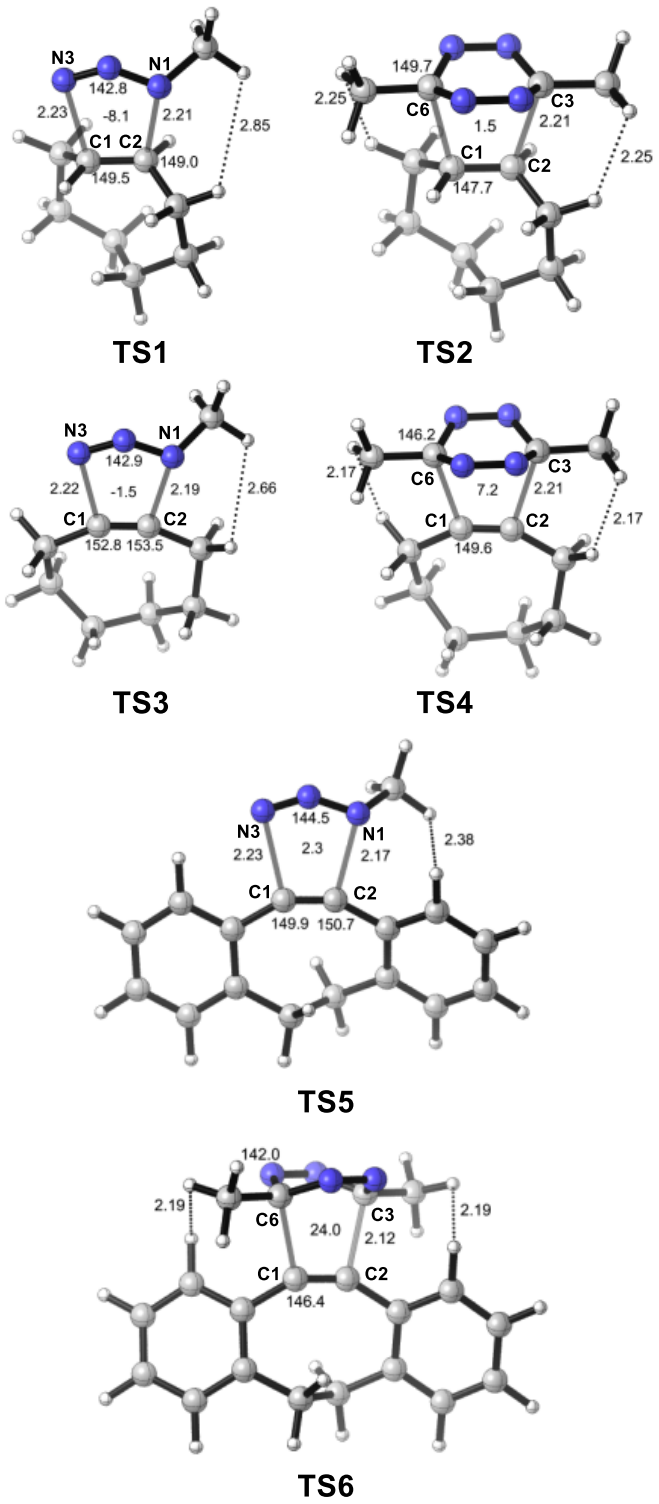

Figure 9. M06-2X/6-311+G(d,p) optimized transition structures of methyl azide-cycloadditions: **TS1** (*trans*-cyclooctene), **TS3** (cyclooctyne), and **TS5** (dibenzocyclooctyne), and dimethyltetrazine-cycloadditions: **TS2** (*trans*-cyclooctene), **TS4** (cyclooctyne), and **TS6** (dibenzocyclooctyne). Distances are given in Å, and angles or dihedral angles are given in degrees.

Trans-cyclooctene, cyclooctyne, and dibenzocyclooctyne are all highly reactive, because their distortion energies (3-6 kcal/mol, **TS1-5**) are much lower than those for unstrained alkenes or alkynes (8-17 kcal/mol).[14j,k] For the cycloadditions of *trans*-cyclooctene, calculations indicate that the activation free energy in water with tetrazine (via transition state **TS2**) is lower than that with azide (via **TS1**) by more than 8 kcal mol^{-1} (Table 1). This accounts for the almost exclusive tetrazine-selectivity of *trans*-cyclooctenes in experiments.[8,9] The distortion/interaction model analysis shows that the distortion energies of transition states **TS1** and **TS2** are nearly identical, but that the favorable interaction energy of **TS2** is much larger than that of **TS1** (-17.8 versus -8.2 kcal mol^{-1}, Table 1). This indicates that the different electronic properties of tetrazine and azide produce this large activation energy difference. The frontier molecular orbital (FMO) analysis (Figure 10) indicates that the preferred orbital interaction is between the HOMO of *trans*-cyclooctene and the LUMO of methyl azide, or relevant vacant orbital of dimethyltetrazine.[53] Notably, azide is a much weaker electron acceptor than tetrazine due to its higher LUMO energy (3.39 versus 2.48 eV, Figure 11). The smaller orbital energy gap between *trans*-cyclooctene and tetrazine makes the favorable orbital interaction in **TS2** stronger than that in **TS1**. Therefore, tetrazines are much more reactive than azides in the cycloadditions using *trans*-cyclooctenes. The reason is the classic origin of high electrophilic reactivity - a low energy vacant orbital.[54]

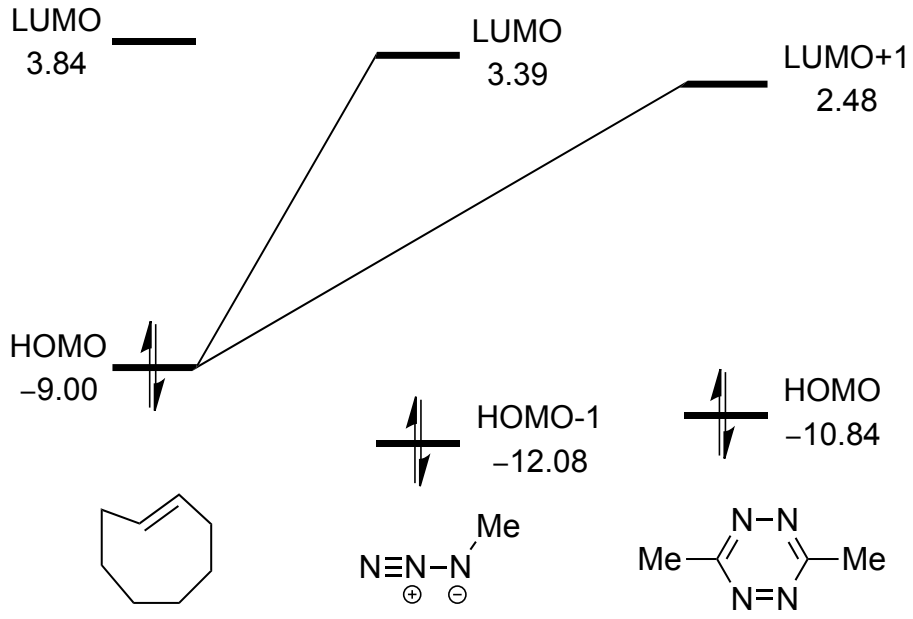

Figure 10. FMO diagram for the cycloadditions of *trans*-cyclooctene with methyl azide and dimethyltetrazine. HF//M06-2X/6-311+G(d,p) computed orbital energies are given in eV.

However, in the cycloadditions of dibenzocyclooctyne, computational results show that dimethyltetrazine reacts 7 orders of magnitude slower than methyl azide (Table 1, **TS5-6**), in good agreement with the experimental observation that dibenzocyclooctyne derivatives only react with azides.[8] The extremely sluggish kinetics of the dibenzocyclooctyne-tetrazine cycloaddition is mainly due to very high distortion energy for this reaction (36.7 kcal mol^{-1}, **TS6**). The structures of transition states **TS5** and **TS6** (Figure 10) show that two distances between the methyl hydrogen atoms of tetrazine and the *ortho* hydrogen atoms of the aromatic rings in **TS6** are only 2.19 Å, shorter than the

sum (2.20 Å) of their van der Waals radii.[55] This indicates that there are strong steric repulsions between dimethyltetrazine and dibenzocyclooctyne. However, the shortest H-H distance between methyl azide and dibenzocyclooctyne is 2.38 Å, implying that the steric repulsion in **TS5** may be ignored. Besides, the N1-N3-C1-C2 dihedral angle in **TS5** is 2.3°, and such a planar geometry ensures the maximum orbital overlap in the cycloaddition transition state. In contrast, the orbital overlap in **TS6** is poor, as evidenced by the C3-C6-C1-C2 dihedral angle of 24°. The combined effects of the unfavorable steric repulsion and the poor orbital overlap greatly move the transition state **TS6** later along the reaction coordinate. A later transition state means a greater geometrical deformation of reactants, requiring more distortion energy. To reach **TS6**, dibenzocyclooctyne needs additional distortion energy of 5.6 kcal mol^{-1} to further bend its bond angle by about 4° with respect to the geometry in **TS5**. The required distortion energy for tetrazine in **TS6** is 10.7 kcal mol^{-1} more than that for azide in **TS5** (27.8 versus 17.1 kcal mol^{-1}, Table 3). The selectivity of dibenzocyclooctyne can be understood by inspecting the space-filling models of reactants and transition states (Figure 11).[56] The steric effects of the *ortho* aryl hydrogen atoms of dibenzocyclooctyne make 3,6-disubstituted tetrazines react dramatically slower than the small azides.

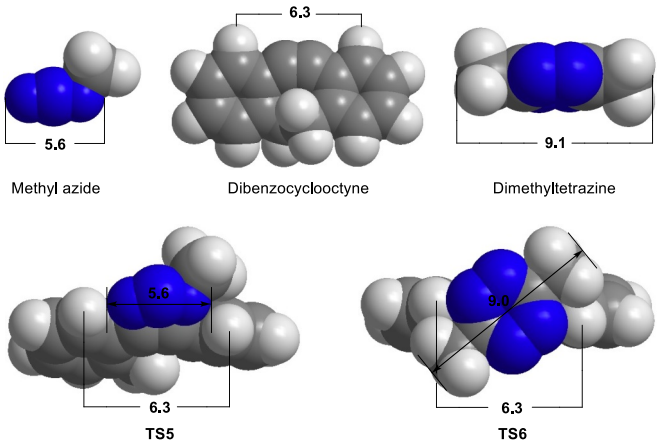

Figure 11. Space-filling models of dibenzycyclooctyne, methyl azide, dimethyltetrazine, and **TS5** and **TS6**. Distances are given in Å.

For the cycloadditions of cyclooctyne, the computed activation free energy for the tetrazine (4+2) reaction (via transition state **TS4**) is 2.6 kcal mol^{-1} lower in water than that for the azide (3+2) reaction (via **TS3**, Table 1). This indicates that the cyclooctyne-tetrazine cycloaddition is only a few orders of magnitude faster than the cyclooctyne-azide cycloaddition. The interaction energy of TS4 is 9.1 kcal/mol greater in magnitude than that of **TS3** (**–** 18.0 vs. **–** 8.9 kcal/mol) because of the favorable electronic effect of tetrazine, but the distortion energy of **TS4** is 5.4 kcal/mol higher than that of **TS3** (26.0 vs. 20.6 kcal/mol) because of steric repulsions between dimethyltetrazine and the propargylic hydrogen atoms of cyclooctyne in **TS4** (Figure 9). We can now propose generalized principles for the design of orthogonal reaction pairs in cycloadditions of the same electron-demand type.[19] The electronically more reactive electrophile (or

nucleophile) A must be sterically more encumbered than the electronically less reactive one B (e.g., A = dimethyltetrazine, B = methyl azide). A reacts more readily with sterically unencumbered cycloaddition partners, but B reacts more readily with sterically encumbered ones. We have used these principles to predict that two new bioorthogonal reagents, methylcyclopropene[3f] and 3,3,6,6-tetramethylthiacycloheptyne,[2c] should also be mutually orthogonal in azide and tetrazine cycloadditions (Scheme 4; the relative rate constants shown are predicted for aqueous solution)

Scheme 4. Prediction of Mutually Orthogonality of Two New Bioorthogonal Reagents in Azide and Tetrazine Cycloadditions.

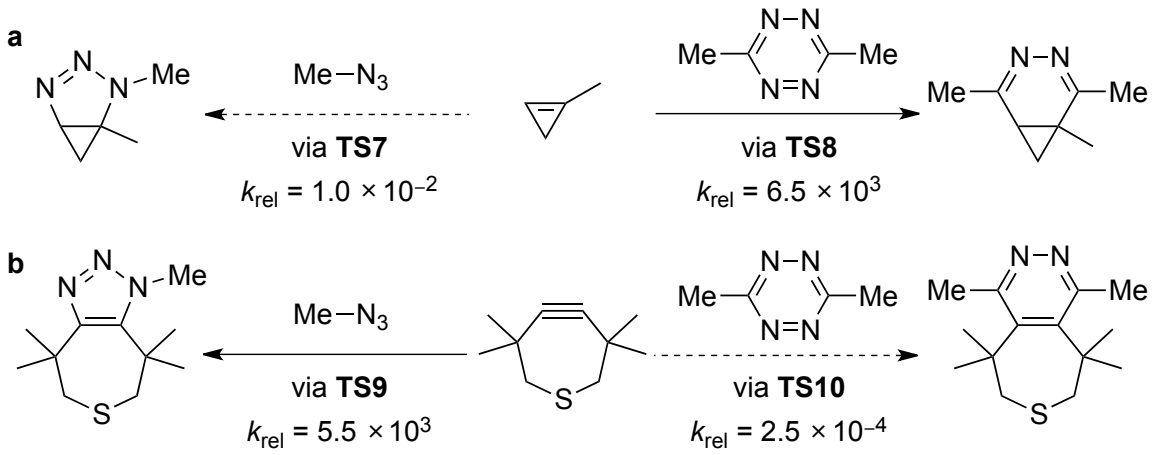

Methylcyclopropene derivatives show high rates of reaction with tetrazines[3f,57] while 3,3,6,6-tetramethylthiacycloheptyne has been found to react readily with azides.[2c] The sterically encumbered but electronically reactive tetrazine should react much faster than the azide with the sterically unencumbered cyclopropene (Scheme 3a), while the azide should be much more reactive with the sterically encumbered cycloalkyne with four methyl groups adjacent to the alkyne moiety (Scheme 3b). The computed activation free energies, relative rate constants, and distortion/interaction energies of the corresponding cycloadditions further support our prediction (**TS7–10** ; Table 3).[58] Further computational design of new bioorthogonal and orthogonal cycloadditions is ongoing in our laboratory.

VI. References

[1] Huisgen, R.; Ooms, P. H. J.; Mingin, M.; Allinger, N. L.; *J. Am. Chem. Soc.* **1980**, 102, 11, 3951-3952.

[2] Huisgen, Rolf. The Adventure Playground of Mechanisms and Novel Reactions. Unilever Research U.S., Inc. Washington, D.C.: American Chemical Society, 1994.

[3] Kolb, H. C.; Finn, M. G.; Sharpless, K. B. *Angew. Chem., Int. Ed.* **2001**, *40*, 2004.

[4] Sletten, E. M.; Bertozzi, C. R. *Acc. Chem. Res.*, **2011**, *44*, 666.

[5] Karver, M. R.; Weissleder, R.; Hilderbrand, S. A.; *Angew. Chem., Int. Ed.* **2012**, *22*, 2263.

[6] Huisgen, R.; *Angew., Chem. Int. Ed. Engl.* **1963**, *2*, 565

[7] Woodward, R. B.; Hoffmann, R.; *J. Am. Chem. Soc.* **1965**, *87*, 395.

[8] Diels. O.; Alder, K. *Liebigs Ann. Chem.* **1928**, *460*, 98

[9] Rondan, N. G.; Paddon-Row, M. N.; Caramella, P.; Houk, K. N. *J. Am. Chem. Soc.* **1981** *103*, 2436.

[10] Watson, W. H.; Galloy, J.; Bartlett, P. D.; Roof, A. A. M.; *J. Org. Chem.* **1985**, *50*, 4093.

[11] Houk, K. N.; Rondan, N. G.; Brown, F. K.; Jorgensen, W. L.; Madura, J. D.; Spellmeyer, D. C. *J. Am. Chem. Soc.* **1983**, *105*, 5980.

[12] Williams, R. V.; Colvin, M. E.; Tran, N.; Warrener, R. N.; Margetic´, D *J. Org. Chem.* **2000**, *65*, 562.

[13] Holthausen, M. C.; Koch, W. *J. Phys. Chem.* **1993**, *97*, 10021.

[14] Volland, W. V.; Davidson, E. R.; Borden, W. T. *J. Am. Chem. Soc.*, **1979** *101*, 533

[15] Saxon, E.; Bertozzi, C. R. *Science* **2007**, *287*, 2007.

[16] Staudinger, H; Meyer, J. *Helv. Chim. Acta.* **1919**, 2, 635.

[17] Frisch, M. J.; et. al. (see complete reference in the Supporting Information). *Gaussian 09*, revision C-01; Gaussian Inc.; Wallingford, CT, 2009.

[18] Zhao, Y.; Truhlar, D. G. *Theor. Chem. Acc.* **2008**, *120*, 215.

[19] (a) Grimme, S. J. *J. Chem. Phys.* **2003**, *109*, 3067. (b) Grimme, S. *J. Chem. Phys.* **2003**, *118*, 9095. (c) Greenkamp, M.; Grimme, S. *Chem. Phys. Lett.* **2004**, *392*, 229.

[20] Canses, E.; Mennucci, J.; Tomasi, J. *J. Chem. Phys.* **1997**, *107*, 3032.

[21] (a) Barone, V.; Cossi, M.; J. Phys. Chem. A, 1998, *102*, 1995-2001. (b) Cossi, M.; Rega, N.; Scalmani, G.; Barone, V. *J. Comp. Chem.* **2003**, *24*, 669.

[22] Zhao, Y.; Truhlar, D. G. *Phys. Chem. Chem. Phys.* **2008**, *10*, 2813.

[23] Ribeiro, R. F.; Marenich, A. V.; Cramer, C. J.; Truhlar, D. G. *J. Phys. Chem. B.* **2011**, *115*, 14556.

[24] Lan, Y.; Zou, L; Cao, Y.; Houk, K. N. *J. Phys. Chem. A* **2011**, *115*, 13906.

[25] Williams, R. V.; Margetić, D. *J. Org. Chem.* **2004**, *69*, 7134.

[26] Fernandez, J. A.; Vazquez, S. *Eur. J. Org. Chem.* **2007**, *27*, 4493.

[27] Ess, D. H.; Houk, K. N. *J. Am. Chem. Soc.*, **2007**, *129*, 10646.

[28] de Jong, G. T.; Bickelhaupt, F. M. *ChemPhysChem* **2007**, *8*, 1170.

[29] Schleyer, P. von R. *J. Am. Chem. Soc.* **1964**, *86*, 1854.

[30] Huisgen, R.; Moebius, L.; Mueller, G.; Stangl, H.; Szeimies, G.; Vernon, J. M. *Chem. Ber.*, **1965**, *98*, 3992.

[31] Watson, W. H.; Galloy, J.; Bartlett, P. D.; Roof, A. A. M. *J. Org. Chem.* **1985**, 50, 4093.

[32] Ess, D. H.; Houk, K. N. *J. Am. Chem. Soc.* **2008**, *130*, 10187.

[33] Jones, G. O.; Houk, K. N. *J. Org. Chem.*, **2008**, *73*, 1333.

[34] Paton, R. S.; Kim, S.; Ross, A. G.; Danishefsky, S. J.; Houk, K. N.; *Angew. Chem., Int. Ed.* **2011**, *50*, 10366.

[35] Fernandez, I.; Cossio, F. P.; Bickelhaupt, F. Matthias *J. Org. Chem.* **2011**, *76*, 2310.

[36] Fernandez, I.; Bickelhaupt, F. Matthias; *J. Comp. Chem.* **2012**, *33*, 509.

[37] Dimroth, O.; *Angewandte Chemie* **1933**, *46*, 571.

[38] Evans, M. G.; Polanyi, M.; *Trans. Faraday Soc.* **1936**, *32*, 1340.

[39] Marcus, R. A.; *J. Chem. Phys.* **1956**, *24*, 966.

[40] Agard, N. J.; Prescher, J. A.; Bertozzi, C. R. *J. Am. Chem. Soc.* **2004**, *126*, 15046.

[41] Kolb, H. C.; Finn, M. G.; Sharpless, K. B. *Angew. Chem., Int. Ed.* **2001**, *40*, 2004.

[42] (a) Agard, N. J.; Prescher, J. A.; Bertozzi, C. R. *J. Am. Chem. Soc.* **2004**, *126*, 15046.

(b) Sletten, E. M.; Bertozzi, C. R. *Acc. Chem. Res.* **2011**, *44*, 666.

[43] (a) Baskin, J. M.; Prescher, J. A.; Laughlin, S. T.; Agard, N. J.; Chang, P. V.; Miller, I. A.; Lo, A.; Codelli, J. A.; Bertozzi, C. R. *Proc. Natl. Acad. Sci. U.S.A.* **2007**, *104*, 16793. (b) Codelli, J. A.; Baskin, J. M.; Agard, N. J.; Bertozzi, C. R. *J. Am. Chem. Soc.* **2008**, *130*, 11486. (c) Ning, X. H.; Guo, J.; Wolfert, M. A.; Boons, G. J. *Angew. Chem., Int. Ed.* **2008**, *47*, 2253. (d) Jewett, J. C.; Sletten, E. M.; Bertozzi, C. R. *J. Am. Chem. Soc.* **2010**, *132*, 3688. (e) Dommerholt, J.; Schmidt, S.; Temming, R.; Hendriks, L. J. A.; Rutjes, F. P. J. T.; van Hest, J. C. M.; Lefeber, D. J.; Friedl, P.; van Delft, F. L. *Angew. Chem., Int. Ed.* **2010**, *49*, 9422. (f) Debets, M. F.; van Berkel, S. S.; Schoffelen, S.; Rutjes, F. P. J. T.; van Hest, J. C. M.; van Delft, F. L. *Chem. Commun.* **2010**, *46*, 97.

[44] (a) Blackman, M. L.; Royzen, M.; Fox, J. M. *J. Am. Chem. Soc.* **2008**, *130*, 13518. (b) Devaraj, N. K.; Weissleder, R.; Hilderbrand, S.A. *Bioconjugate Chem.* **2008**, *19*, 2297.

[45] Karver, M. R.; Weissleder, R.; Hilderbrand, S. A. *Bioconjugate Chem.* **2011**, *22*, 2263.

[46] Plass, T.; Milles, S.; Koehler, C.; Szymanski, J.; Mueller, R.; Wiebler, M.; Schultz, C.; Lemke, E. A. *Angew. Chem., Int. Ed.* **2012**, *51*,4166.

[47] Karver, M. R.; Weissleder, R.; Hilderbrand, S. A. Angew. Chem., Int. Ed. **2012**, *51*, 920.

[48] (a) Agard, N. J.; Baskin, J. M.; Prescher, J. A.; Lo, A.; Bertozzi, C. R. *ACS Chem. Biol.* **2006**, *1*, 644. (b) Chen, W.; Wang, D.; Dai, C.;Hamelberg, D.; Wang, B. *Chem. Commun.* **2012**, *48*, 1736.

[49] Frisch, M. J.; et al. Gaussian 09, revision C.01; Gaussian, Inc.: Wallingford, CT, 2010.

[50] (a) Zhao, Y.; Truhlar, D. G. *Theor. Chem. Acc.* **2008**, *120*, 215. (b) Zhao, Y.; Truhlar, D. G. *Acc. Chem. Res.* **2008**, *41*, 157.

[51] (a) Paton, R. S.; Mackey, J. L.; Kim, W. H.; Lee, J. H.; Danishefsky, S. J.; Houk, K. N. *J. Am. Chem. Soc.* **2010**, *132*, 9335. (b) Lan, Y.; Zou, L.; Cao, Y.; Houk, K. N. *J. Phys. Chem. A* **2011**, *115*, 13906.

[52] (a) Ess, D. H.; Houk, K. N. *J. Am. Chem. Soc.* **2007**, *129*, 10646. (b) Ess, D. H.; Houk, K. N. *J. Am. Chem. Soc.* **2008**, *130*, 10187. (c) Hayden, A. E.; Houk, K. N. *J. Am. Chem. Soc.* **2009**, *131*, 4084. (d) Schoenebeck, F.; Ess, D. H.; Jones, G. O.; Houk, K. N. *J. Am. Chem. Soc.* **2009**, *131*, 8121. (e) van Zeist, W.-J.; Bickelhaupt, F. M. *Org. Biomol. Chem.* **2010**, *8*, 3118. (f) Fernández, I.; Cossío, F. P.; Bickelhaupt, F. M. *J. Org. Chem.* **2011**, *76*, 2310. (g) Lan, Y.; Wheeler, S. E.; Houk, K. N. *J. Chem. Theory Comput.* **2011**, *7,* 2104. (h) Paton, R. S.; Kim, S.; Ross, A. G.; Danishefsky, S. J.; Houk, K. N. *Angew. Chem., Int. Ed.* **2011**, *50*, 10366. (i) Fernández, I.; Bickelhaupt, F. M. *J. Comput. Chem.* **2012**, *33*, 509. (j) Gordon, C. G.; Mackey, J. L.; Jewett, J. C.; Sletten, E. M.; Houk, K. N.; Bertozzi, C. R. *J. Am. Chem. Soc.* **2012**, *134*, 9199. (k) Lopez, Steven Alexander; Houk, K. N. *J. Org. Chem.* **2012**, DOI: 10.1021/jo301267b.

[53] In the cycloadditions of strained alkynes, FMO analysis showed that charge transfer from the alkyne to methyl azide or dimethyltetrazine also occurs.

[54] Houk, K. N. *Acc. Chem. Res.* **1975**, *8*, 361.

[55] Rowland, R. S.; Taylor, R. *J. Phys. Chem.* **1996**, *100*, 7384.

[56] As shown in Figure 3, the two ortho hydrogen atoms of the aromatic rings in dibenzocyclooctyne form a 6.3 Å wide "gate" in the front of the carbon–carbon triple bond. Because the methyl group is not aligned with the two reacting nitrogen atoms of the azide, the effective size of methyl azide is 5.6 Å. Such a size can be accepted well by the 6.3 Å wide gate of dibenzocyclooctyne. In contrast, the two methyl groups and two reacting carbon atoms of the tetrazine are all in a straight line, so the effective size of dimethyltetrazine is up to 9.1 Å. Obviously, the 6.3 Å wide gate of dibenzocyclooctyne is so narrow that dimethyltetrazine has to twist to react.

[57] Thalhammer, F.; Wallfahrer, U.; Sauer, J. *Tetrahedron Lett.* **1990**, *31*, 6851.

[58] The activation free energy for the generation of the regioisomer (via TS7a) from methylcyclopropene and methyl azide in water is 29.7 kcal/mol.